ACS OMEGA

http://pubs.acs.org/journal/acsodf

Article

Rod-Shaped β-FeOOH Synthesis for Hydrogen Production under Light Irradiation

Younghwa Yoon, Ken-ichi Katsumata, Norihiro Suzuki, Kazuya Nakata, Chiaki Terashima, Kyung Hwan Kim, Akira Fujishima, and Jeongsoo Hong*

Cite This: *ACS Omega* 2021, 6, 30562−30568

Read Online

ACCESS | Metrics & More | Article Recommendations | Supporting Information

ABSTRACT: Renewable energy is spotlighted as a resource to replace fossil fuels, and among the resources, active research on hydrogen energy is ongoing. Various methods have been developed to produce hydrogen energy using photoreduction processes. In this study, we synthesized β-phase iron oxyhydroxide (β-FeOOH) using a hydrothermal method with an optimal synthesis time and investigated its photofunctional properties, including hydrogen production. The obtained samples were characterized and compared with reference data. X-ray powder diffraction results corresponded to the peaks of the reference data. A rod structure was confirmed by scanning electron microscopy, and no impurities were observed. The band-gap energy of β-FeOOH was calculated as 1.8−2.6 eV. A photoreduction process was performed based on a photo-Fenton reaction to produce hydrogen by irradiating ultraviolet (UV) on β-FeOOH. The synthesized β-FeOOH was subjected to UV irradiation for 24 h to produce hydrogen, and we confirmed that hydrogen was successfully produced. The properties of β-FeOOH were evaluated after UV irradiation.

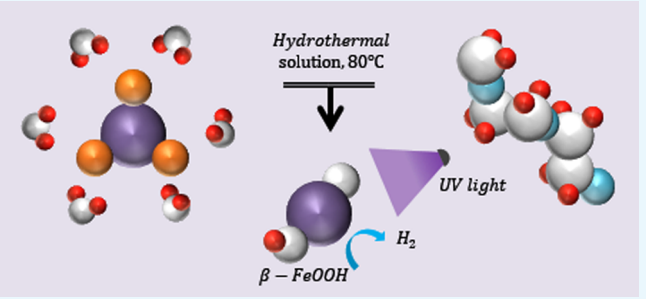

INTRODUCTION

The adverse effects of environmental problems, such as global warming and air pollution, resulting from the use of fossil fuels, have prompted the search for alternative energy sources. Renewable energy, capable of sustainable growth, has become the focus of global research as an alternative to fossil fuels. Hydrogen as a fuel does not emit environmentally harmful pollutants; hence, research is ongoing to increase hydrogen production as a clean energy source to solve the environmental problems posed by fossil fuels.[1]

Among the various methods of hydrogen production,[2,3] photocatalysis, which uses light to accelerate the photoreaction of photocatalysts, has been extensively studied.[4] Photocatalysis is a reaction in which electrons are excited in the valence band by irradiating light with sufficient energy to metal oxide and the electrons excited in the conduction band react with materials present on the photocatalyst surface.[5−8]

In this study, we investigated metal oxide materials that are not widely used and can be recycled. Among various resources, rust was devised, which is a very common material on earth, and a waste readily available at a low cost, and yet not fully utilized. Rusty iron is an iron oxide and has various bonding forms. Fe_2O_3 and Fe_3O_4 are representative oxides, and several studies have been reported on producing ecofriendly hydrogen for applications in water purification and air pollution control.[9,10] Herein, we discovered iron oxyhydroxide (FeOOH) among various iron oxides, which has not been used for hydrogen generation. FeOOH has four crystal phases including α—(goethite), β—(akaganeite), γ—(lepidocrocite), and δ—(ferroxyhyte), with band-gap energies ranging from 1.8 to 2.3 eV. Thus, it can only absorb visible light with a wavelength of 380−750 nm.[11] β-FeOOH has been synthesized using hydrothermal methods[12] and investigated under varying experimental conditions, including the treatment time, to find the optimal synthesis time (Figure S1).

As-synthesized β-FeOOH was initially used in the experiment, which requires 1.2 eV for oxygen and hydrogen to undergo redox reactions.[13] However, the experiment was unsuccessful due to the insufficient energy exhibited by β-FeOOH.[14,15] Thus, β-FeOOH could only be used as a buffer layer to absorb visible light during electrolysis by integrating electrochemical fields.[16,17] In this case, an applied voltage is required and visible light is irradiated on a thin film.[18] However, although FeOOH absorbs visible light, the energy of visible light is insufficient to generate hydrogen; hence, FeOOH cannot function as a photocatalyst. Here, we developed a unique hydrogen production method based on

Received: August 8, 2021
Accepted: October 28, 2021
Published: November 4, 2021

photo-Fenton reactions. The process using β-FeOOH was carried out under UV irradiation without applying a voltage, and the temperature was varied to examine the effect on hydrogen production. We expected that hydrogen production would be possible due to the reaction under UV irradiation. The Fenton (eq 1) and photo-Fenton (eq 2) reactions are expressed as follows[19,20]

$$Fe^{2+} + H_2O_2 \rightarrow {}^{\cdot}OH + Fe^{3+} + OH^- \quad (1)$$

$$Fe(OH)^{2+} + h\nu \rightarrow Fe^{2+} + {}^{\cdot}OH \quad (2)$$

EXPERIMENTAL SECTION

Iron(III) chloride hexahydrate ($FeCl_3{\cdot}6H_2O$, ferric chloride), >99.0%, Wako) and poly(ethylene glycol) (PEG, H-$(OCH_2CH_2)_n$OH, #10000, Yakuri) were purchased for β-FeOOH synthesis. Methanol (CH_3OH, >99.8%, Wako) was purchased for the hydrogen procedure. Double deionized (DI) water was used in all of the procedures. β-FeOOH was synthesized by employing ferric chloride as a primary reductant and PEG as a secondary reductant. The reduction process was carried out at room temperature (RT), i.e., 21 °C. β-FeOOH was investigated by varying the experimental conditions of its synthesis. The hydrothermal treatment time was varied, as shown in Table 1. A typical procedure is as follows: the required volumes of freshly prepared aqueous solutions containing $FeCl_3$ and PEG were mixed in 40 mL of DI water for 5 min by stirring to ensure a homogeneous solution. The solutions were then heated to 80 °C in an oven using hydrothermal treatment (Table 2).

Table 1. Hydrothermal Treatment Time Conditions for Finding Optimal Synthesis Time

no.	synthesis time (h)	treatment temperature (°C)	primary reductant	secondary reductant
#1	3	80	ferric chloride	PEG (10000)
#2	6			
#3	12			
#4	24			

Table 2. Hydrogen Production by Irradiating UV in a Dark State

temperature	UV intensity	solvent	β-FeOOH
RT 80 °C	2.5 mW/cm^2	DI water + methanol (9:1)	50 mg

The structural properties of the synthesized β-FeOOH were observed by X-ray diffraction (XRD, MPA-2000, Rigaku) at 20−80° and scanning electron microscopy (SEM, S-4700, Hitachi). UV−vis extinction spectra were recorded using a spectrophotometer (Lambda 750 UV−vis−NIR, Perkin Elmer) in the absorbance mode (190−1400 nm). As the crystal structure collapses and reacts with oxygen, it is circulated to FeOOH.

Hydrogen production was conducted by adding the synthesized β-FeOOH to prepared aqueous solutions containing DI water and methanol under UV irradiation, with the intensity fixed at 2.5 mW/cm^2. The process was conducted in the dark at RT and 80 °C. The amount of hydrogen produced was measured with a gas chromatography-thermal conductivity detector (GC-TCD-2014, Shimadzu).

RESULTS AND DISCUSSION

The initial pH of the synthesized β-FeOOH under various hydrothermal treatment times was 3.59. Figure 1 shows the SEM images of the as-synthesized β-FeOOH, and they all reveal rod-like structures. The size of β-FeOOH particles increased with the synthesis time (a = height: 500−537 nm, width: 175−200 nm; b = height: 750−762 nm, width: 187−212 nm; c = height: 930−950 nm, width: 220−250 nm). Growth on the preferential growth plane controlling the length was confirmed by the X-ray diffraction (XRD) pattern.

In the XRD patterns (Figure 2), all peaks of the as-synthesized samples are attributed to akaganeite (JCPDS 34-1266), and no impurities were observed. However, the peak intensities varied with the hydrothermal treatment time. The sample with a hydrothermal time of 6 h showed broad peaks, whereas those of the samples with hydrothermal times of 12 and 24 h were sharp. The preferential growth plane of the rod-structured particles was the (310) peak, which is responsible for the particle length.

The crystallite size was calculated using the Scherrer equation with (310) peak data from the XRD patterns (see the Supporting Information, Figure S1),[21] which is expressed as

$$\tau = \frac{K\lambda}{\beta \cos\theta} \quad (3)$$

In eq 3, β is the full-width at half maximum (FWHM), which is inversely related to the crystallite size τ. Therefore, the larger FWHM, i.e., the broader the XRD pattern, the smaller the crystallite size. As shown in Figure S1 (see the Supporting Information), considering the (310) peak, the crystallite size varied with the synthesis time (#1: 32.5 nm, #2: 34.7 nm, #3: 49.4 nm). We infer that there is a correlation between the specific surface area and the average crystallite size: the smaller the crystallite size, the larger the specific surface area, which favors the hydrogen evolution reaction (HER).[22] Therefore, the sample having a broad XRD pattern has a large specific surface area, favoring redox reactions.[23] Among the four samples, the 6 h sample was used for hydrogen because of the relationship between the particle size and the surface area, which indicates that the sample with smaller crystallites has a large specific surface area. The large specific surface area indicates high redox reaction efficiency, resulting in a positive effect on hydrogen production.[24,25]

The optical characteristics of the as-synthesized samples were measured (see the Supporting Information, Figure S2). The absorbance was measured in a wavelength range of 200−1400 nm, and we calculated the range of wavelengths to ensure that β-FeOOH absorbed only visible-light wavelengths. β-FeOOH absorbed only radiation in the visible spectrum, implying that visible light can be used for the redox reaction. The band-gap energy (E_g) of the four samples was calculated using the Kubelka−Munk method as one of the diffuse reflectance measurements. The band gap of the samples ranged from 1.9 to 2.2 eV, which is consistent with that reported for β-FeOOH.[26] According to the relationship between particle size and HER, the smaller the particle size, the larger the HER.[27]

The photo-Fenton reaction was conducted employing UV irradiation in the Fenton process for photoreduction of Fe^{3+} to

https://doi.org/10.1021/acsomega.1c04251
ACS Omega 2021, 6, 30562−30568

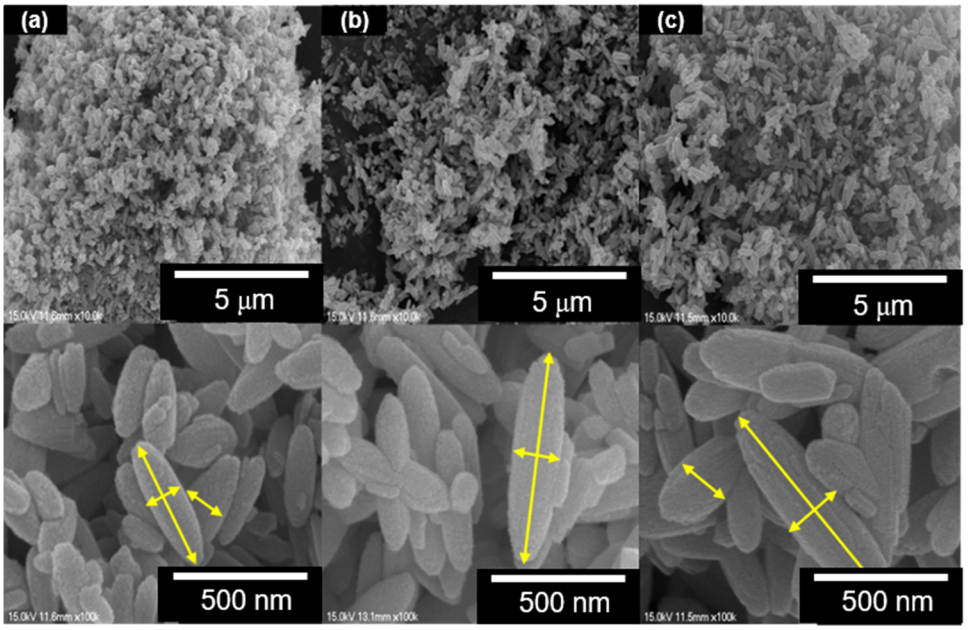

Figure 1. SEM images of as-synthesized β-FeOOH at different synthesis times: (a) 6 h (height: 500−537 nm, width: 175−200 nm), (b) 12 h (height: 750−762 nm, width: 187−212 nm), and (c) 24 h (height: 930−950 nm, width: 220−250 nm).

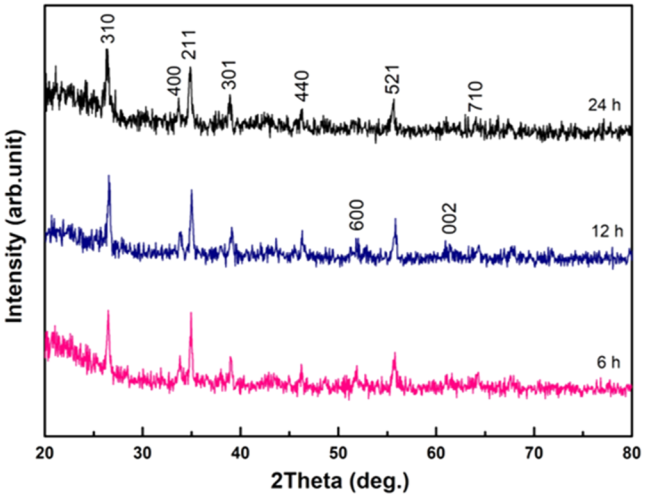

Figure 2. X-ray diffraction patterns of as-synthesized β-FeOOH at different hydrothermal times.

Fe^{2+}. A redox couple consisting of water and ferrous ion was used. The process is expressed as follows[28−31]

$$Fe^{3+} + H_2O \xrightarrow{h\nu} Fe^{2+} + H^+ + {}^{\cdot}OH \ (\lambda<530\ nm) \quad (4)$$

$$4Fe^{2+} + O_2 + 4H^+ \rightarrow 4Fe^{3+} + 2H_2O \ (\text{in acid condition}) \quad (5)$$

When UV light is used in eq 4, electrons in the valence band are excited and holes are generated, and Fe^{3+} is reduced to Fe^{2+}. The generated holes decompose H_2O into H^+ and $^{\bullet}OH$. The efficiency of the photo-Fenton reaction process is determined by the reactivity of $^{\bullet}OH$ radicals. In eq 5, the electrons from Fe^{2+} participate in the formation of H_2O and are oxidized back to Fe^{3+}. In addition, H^+ produced in eq 4 is expected to be involved in three reactions reacting with $^{\bullet}OH$ to form H_2O, or reacting with oxygen in the atmosphere to become H_2O, or generating electrons to produce hydrogen. β-FeOOH can be circulated by the abovementioned reactions. During the circulation of β-FeOOH, hydrogen is produced (Scheme 1).[32]

Scheme 1. Hydrogen Production Process under UV Irradiation

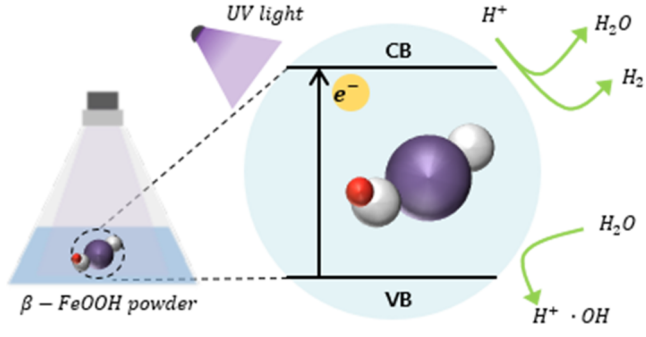

As shown in Figure S2 (see the Supporting Information), β-FeOOH absorbed only visible light, but reactions occurred upon UV irradiation to produce hydrogen, which is attributed to the photo-Fenton reactions. The solution was prepared in a water to methanol ratio of 9:1, and the pH was 3.59.

Before proceeding with the hydrogen generation experiment through UV irradiation, two blank experiments were conducted. Both experiments were classified by whether methanol was added to the solution, and were conducted in a dark room. Because photo-Fenton reactions are caused by the excitation of electrons by light energy, both experiments conducted in the dark did not generate hydrogen regardless of methanol.

Hydrogen production was conducted at room temperature (RT) and 80 °C under both visible light and UV irradiation, respectively, to prove that hydrogen is not produced under visible light. The temperature conditions were varied to observe the effect of methanol, an organic solvent constituting the solution. To completely vaporize methanol in the solution,

https://doi.org/10.1021/acsomega.1c04251
ACS Omega 2021, 6, 30562−30568

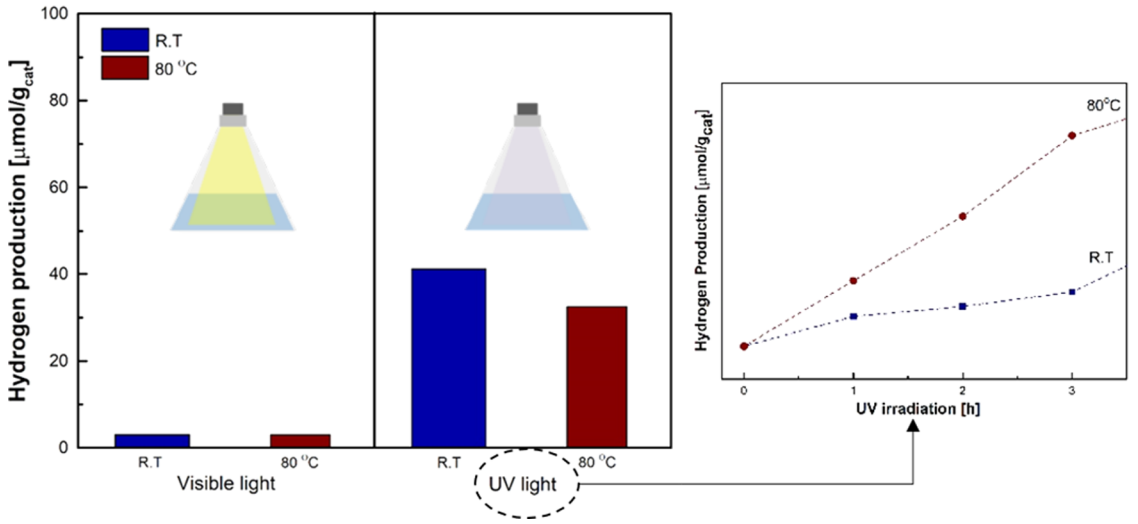

Figure 3. Amount of hydrogen produced at RT and 80 °C under visible and UV irradiation after 24 h.

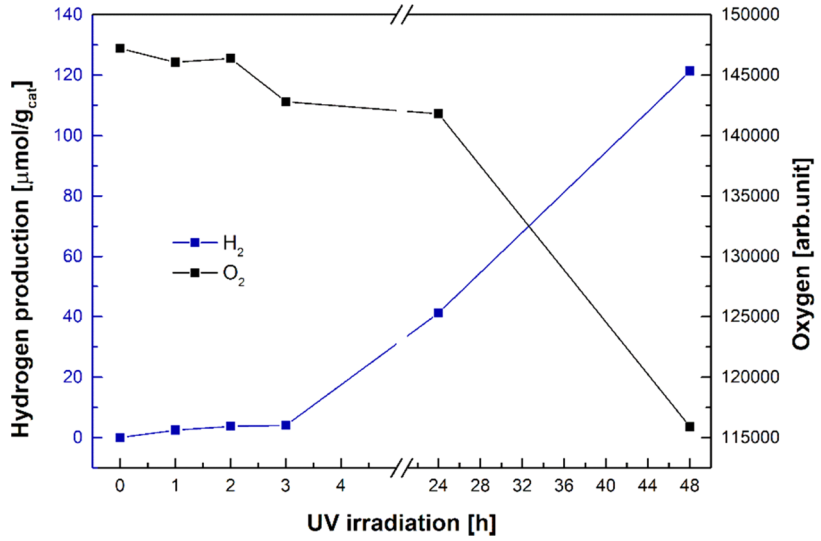

Figure 4. Sustainability of hydrogen production and oxygen consumption over 48 h.

the temperature for the comparative experiment was set to 80 °C, which is higher than the boiling point of methanol (64.7 °C). The temperature of the comparative experiment was set below 100 °C because it is difficult to determine whether the change in hydrogen production is due to the evaporation of methanol or water. Hydrogen generation under visible light and UV irradiation was compared, and the effect of temperature on hydrogen generation was evaluated (Figure 3). After irradiation for 24 h, as expected, no additional hydrogen was found under visible light, but in contrast, hydrogen was generated under UV irradiation.

At the beginning of UV irradiation, more hydrogen was produced at 80 °C, but at the end of the 24 h experiment, the amount of hydrogen produced at RT (41.2 μmol) was higher than that produced at 80 °C (32.5 μmol). Thus, we confirmed that hydrogen production is possible at both RT and 80 °C under UV irradiation.

Measurements after 24 h confirmed that more hydrogen was produced at RT, and the difference between the amount of hydrogen produced at 80 °C and RT is related to the synthesis temperature of β-FeOOH during hydrothermal treatment. β-FeOOH was prepared by hydrothermal treatment at 80 °C. Hydrogen generation experiments at 80 °C showed that the synthesis temperature of the sample causes the aggregation of FeOOH particles, so the specific surface area decreases, and consequently, the reactivity decreases.

A further experiment was performed over a longer period to confirm the feasibility of hydrogen production using FeOOH. Experiments conducted at RT for 48 h showed a steady increase in the amount of hydrogen produced (Figure 4), and semipermanent hydrogen production is possible as long as the FeOOH cycle continues.

Moreover, according to eq 4, oxygen is consumed to recover Fe^{3+}, and Figure 4 shows a reduction of oxygen in the sealed container during the 48 h hydrogen generation experiment. The amount of oxygen after 48 h was significantly decreased compared to the initial amount. Based on this result, oxygen is certainly consumed in photo-Fenton reaction cycles.

The structural characteristics of the samples after UV irradiation are shown in Figures S3 (see the Supporting Information), 4, and 5. The peaks of β-FeOOH after hydrogen production remained the same as those of β-FeOOH before UV irradiation (see the Supporting Information, Figure S3). The peak intensities in the XRD patterns of RT and 80 °C

https://doi.org/10.1021/acsomega.1c04251
ACS Omega 2021, 6, 30562−30568

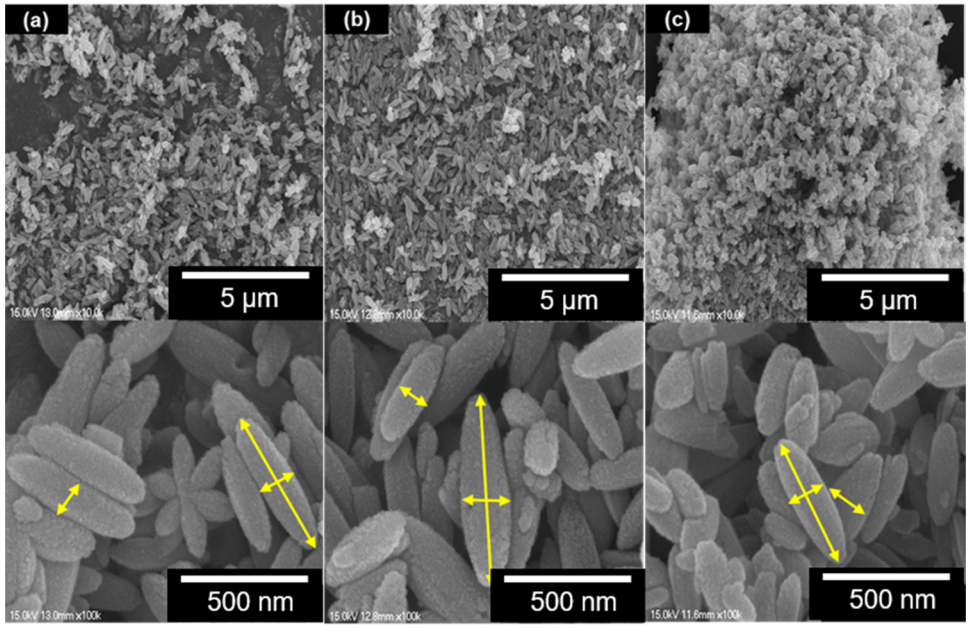

Figure 5. SEM image of β-FeOOH after hydrogen production experiments at various temperatures: (a) RT (height: 500−540 nm, width: 150−185 nm), (b) 80 °C (height: 490−525 nm, width: 162−198 nm), and (c) before UV irradiation (height: 500−537 nm, width: 175−200 nm).

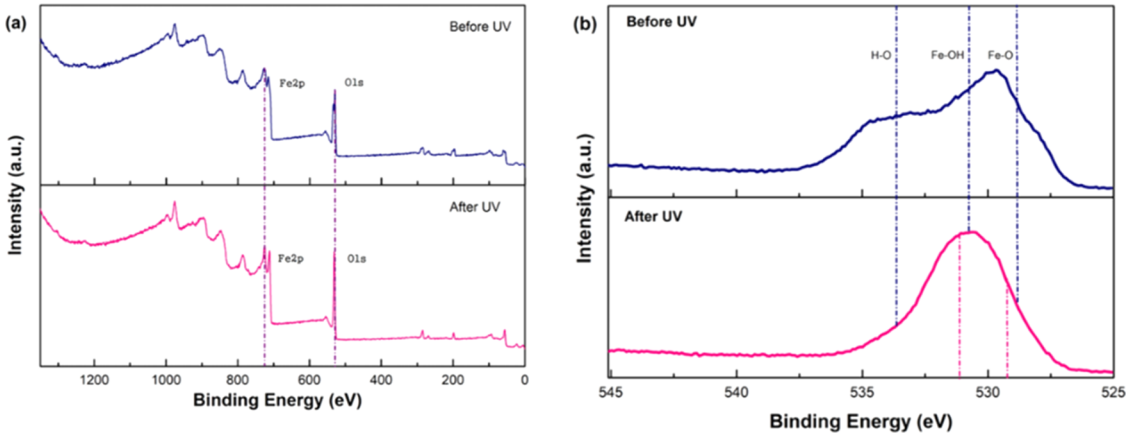

Figure 6. XPS spectra and O 1s core-level spectra of β-FeOOH before and after UV irradiation. (a) Survey scan spectra and (b) O 1s core-level spectra.

samples after the reaction are similar to those before the reaction, and all major peaks were retained but their intensities decreased. Comparing the intensities, we found that the 80 °C sample had better crystallinity than the RT sample, which implies that the 80 °C sample had a larger crystallite size. In particular, more hydrogen would be produced at RT according to the abovementioned data (see the Supporting Information, Figure S1).

As shown in Figure 5, β-FeOOH showed a rod-like structure before and after UV irradiation, and there was no significant difference in the width and the length. Transmission electron microscopy images of the sample also showed a rod-like structure (see the Supporting Information, Figure S4). The appearance of the same peaks and rod structure after irradiation indicates that no noticeable change occurred, except for a decrease in intensity, after hydrogen production. We confirmed that the phase of β-FeOOH was maintained. Thus, we infer that the structural characteristics of β-FeOOH are not affected by UV irradiation and temperature.

XPS spectra of β-FeOOH were recorded before and after UV irradiation (Figure 6).[33,34] Figure 6a shows the survey scan spectra of β-FeOOH, and Figure 6b reveals the presence of H−O, Fe−OH, and Fe−O bonds before UV irradiation. However, after UV irradiation, the intensity of H−O decreases. The peaks of the H−O bond were expected to decrease during the cycle of FeOOH, during which Fe^{2+} photoreduced by UV irradiation is reoxidized to Fe^{3+} according to the above-mentioned photo-Fenton reaction. Further research is required for an accurate interpretation of this data.

Hydrogen production was a result of the photo-Fenton reaction, which is one of the redox reactions that occur under UV irradiation. This reaction upon irradiation is mainly due to the photochemical reduction of Fe^{3+} to Fe^{2+}, which is the major catalytic species in eq 2. During the photo-Fenton reaction, OH^- and H^+ were also produced simultaneously. Then, the Fe^{2+} ions were oxidized in air to Fe^{3+} ions, which supports the results shown in Figure 3.

Since this process consumes only small quantities of FeOOH and produces no additional contaminants, it is a

https://doi.org/10.1021/acsomega.1c04251
ACS Omega 2021, 6, 30562−30568

good hydrogen production method without environmental pollution.[35]

CONCLUSIONS

β-FeOOH was synthesized by a hydrothermal method with varying treatment times, and its structural and optical properties were evaluated. The XRD patterns show the same peaks as the reference data and rod-like structure. Based on the broadness of the XRD patterns and the particle size from the SEM images, the sample synthesized for 6 h is suitable for hydrogen generation. Hydrogen was produced under UV irradiation at varying temperatures, and the structural properties of β-FeOOH after UV irradiation were re-evaluated. The amounts of produced hydrogen were 41.2 and 32.5 μmol at RT and 80 °C, respectively.

ASSOCIATED CONTENT

Supporting Information

The Supporting Information is available free of charge at https://pubs.acs.org/doi/10.1021/acsomega.1c04251.

Analytical data, (Figure S1) crystallite size of as-synthesized β-FeOOH, (Figure S2) optical properties of as-synthesized β-FeOOH, (Figure S3) XRD pattern of β-FeOOH after UV irradiation, and (Figure S40) TEM image of β-FeOOH after the hydrogen production experiment (PDF)

AUTHOR INFORMATION

Corresponding Author

Jeongsoo Hong − *Department of Electrical Engineering, Gachon University, Seongnam, Gyeonggi 13120, Korea;* orcid.org/0000-0002-5946-7815; Email: hongjs@gachon.ac.kr

Authors

Younghwa Yoon − *Department of Electrical Engineering, Gachon University, Seongnam, Gyeonggi 13120, Korea*

Ken-ichi Katsumata − *Photocatalysis International Research Center, Tokyo University of Science, Noda-shi, Chiba-ken 278-8510, Japan;* orcid.org/0000-0002-3841-5354

Norihiro Suzuki − *Photocatalysis International Research Center, Tokyo University of Science, Noda-shi, Chiba-ken 278-8510, Japan;* orcid.org/0000-0002-7154-3892

Kazuya Nakata − *Graduate School of Bio-Applications and Systems Engineering, Tokyo University of Agriculture and Technology, Koganei, Tokyo 184-0012, Japan*

Chiaki Terashima − *Photocatalysis International Research Center, Tokyo University of Science, Noda-shi, Chiba-ken 278-8510, Japan;* orcid.org/0000-0002-8874-1481

Kyung Hwan Kim − *Department of Electrical Engineering, Gachon University, Seongnam, Gyeonggi 13120, Korea*

Akira Fujishima − *Photocatalysis International Research Center, Tokyo University of Science, Noda-shi, Chiba-ken 278-8510, Japan*

Complete contact information is available at: https://pubs.acs.org/10.1021/acsomega.1c04251

Notes

The authors declare no competing financial interest.

ACKNOWLEDGMENTS

This study was supported by the Korea Institute of Energy Technology Evaluation and Planning (KETEP), the Ministry of Trade, Industry & Energy (MOTIE) of the Republic of Korea (No. 20194030202290), and the Gachon University research fund of 2018 (GCU-2018-0286).

REFERENCES

(1) Momirlan, M.; Veziroglu, T. N. The properties of hydrogen as fuel tomorrow in sustainable energy system for a cleaner planet. *Int. J. Hydrogen Energy* **2005**, *30*, 795−802.

(2) Fujishima, A.; Honda, K. Electrochemical photolysis of water at a semiconductor electrode. *Nature* **1972**, *238*, 37−38.

(3) Asahi, R.; Morikawa, T.; Ohwaki, T.; Aoki, K.; Taga, Y. Visible-light photocatalysis in nitrogen-doped titanium oxides. *Science* **2001**, *293*, 269−271.

(4) Ashokkumar, M. An overview on semiconductor particulate systems for photoproduction of hydrogen. *Int. J. Hydrogen Energy* **1998**, *23*, 427−438.

(5) Wang, K.; Jiang, L.; Wu, X.; Zhang, G. Vacancy mediated Z-scheme charge transfer in a 2D/2D $La_2Ti_2O_7$/g-C_3N_4 nanojunction as a bifunctional photocatalyst for solar-to-energy conversion. *J. Mater. Chem. A* **2020**, *8*, 13241−13247.

(6) Jiang, L.; Li, J.; Wang, K.; Zhang, G.; Li, Y.; Wu, X. Low boiling point solvent mediated strategy to synthesize functionalized monolayer carbon nitride for superior photocatalytic hydrogen evolution. *Appl. Catal., B* **2020**, *260*, No. 118181.

(7) Xiao, H.; Liu, P.; Wang, W.; Ran, R.; Zhou, W.; Shao, Z. Ruddlesden-Popper Perovskite Oxides for Photocatalysis-Based Water Splitting and Wastewater Treatment. *Energy Fuels* **2020**, *34*, 9208−9221.

(8) Wang, W.; Tadé, M. O.; Shao, Z. Nitrogen-doped simple and complex oxides for photocatalysis: a review. *Prog. Mater. Sci.* **2018**, *92*, 33−63.

(9) Qian, X.; Ren, M.; Zhu, Y.; Han, Y.; Jia, J.; Zhao, Y.; et al. Visible light assisted heterogeneous Fenton-like degradation of organic pollutant via α-FeOOH/mesoporous carbon composites. *Environ. Sci. Technol.* **2017**, *51*, 3993−4000.

(10) Jiang, Z.; Sun, H.; Wang, T.; Wei, B.; Li, H.; Wong, P. K.; et al. Nature-based catalyst for visible-light-driven photocatalytic CO 2 reduction. *Energy Environ. Sci.* **2018**, *11*, 2382−2389.

(11) White, A. F. Mineral-Water Interface Geochemistry: Reviews. *Rev. Mineral Geochem.* **1990**, *23*, 467−555.

(12) Wang, X.; Chen, X.; Gao, L.; Zheng, H.; Ji, M.; Tang, C.; Shen, T.; Zhang, Z. Synthesis of β-FeOOH and α-Fe_2O_3 nanorods and electrochemical properties of β-FeOOH. *J. Mater. Chem.* **2004**, *14*, 905−907.

(13) Navarro, R. M.; Sánchez-Sánchez, M. C.; Alvarez-Galvan, M. C.; del Valle, F.; Fierro, J. L. G. Hydrogen production from renewable sources: biomass and photocatalytic opportunities. *Energy Environ. Sci.* **2009**, *2*, 35−54.

(14) Wang, M.; Chen, L.; Sun, L. Recent progress in electrochemical hydrogen production with earth-abundant metal complexes as catalysts. *Energy Environ. Sci.* **2012**, *5*, 6763−6778.

(15) Sherman, D. M. Electronic structures of iron (III) and manganese (IV)(hydr) oxide minerals: Thermodynamics of photochemical reductive dissolution in aquatic environments. *Geochim. Cosmochim. Acta* **2005**, *69*, 3249−3255.

(16) Kim, J. Y.; Magesh, G.; Youn, D. H.; Jang, J. W.; Kubota, J.; Domen, K.; Lee, J. S. Single-crystalline, wormlike hematite photo anodes for efficient solar water splitting. *Sci. Rep.* **2013**, *3*, No. 2681.

(17) Vequizo, J. J. M.; Ichimura, M. Fabrication of Cu2O/γ-FeOOH heterojunction solar cells using electrodeposition. *Appl. Phys. Express* **2014**, *7*, No. 045501.

(18) Chemelewski, W. D.; Lee, H. C.; Lin, J. F.; Bard, A. J.; Mullins, C. B. Amorphous FeOOH oxygen evolution reaction catalyst for photoelectrochemical water splitting. *J. Am. Chem. Soc.* **2014**, *136*, 2843−2850.

(19) Wu, K.; Xie, Y.; Zhao, J.; Hidaka, H. Photo-Fenton degradation of a dye under visible light irradiation. *J. Mol. Catal. A: Chem.* **1999**, *144*, 77−84.
(20) Tokumura, M.; Morito, R.; Kawase, Y. Photo-Fenton process for simultaneous colored wastewater treatment and electricity and hydrogen production. *Chem. Eng. J.* **2013**, *221*, 81−89.
(21) Scherrer, P. Nanoscience and the Scherrer equation versus the Scherrer-Gottingen equation. *Nach. Ges. Wiss. Gött.* **1918**, *26*, 98−100.
(22) Bensaid, S.; Piumetti, M.; Novara, C.; Giorgis, F.; Chiodini, A.; Russo, N.; Fino, D. Catalytic oxidation of CO and soot over Ce-Zr-Pr mixed oxides synthesized in a multi-inlet vortex reactor: effect of structural defects on the catalytic activity. *Nanoscale Res. Lett.* **2016**, *11*, No. 494.
(23) Langford, J.; Wilson, A.J.C. Scherrer after sixty years: a survey and some new results in the determination of crystallite size. *J. Appl. Crystallogr.* **1978**, *11*, 102−113.
(24) Yamamoto, O. Influence of particle size on the antibacterial activity of zinc oxide. *Int. J. Inorg. Mater.* **2001**, *3*, 643−646.
(25) Abbott, D. F.; Lebedev, D.; Waltar, K.; Povia, M.; Nachtegaal, M.; Fabbri, E.; Schmidt, T. J.; et al. Iridium oxide for the oxygen evolution reaction: correlation between particle size, morphology, and the surface hydroxo layer from operando XAS. *Chem. Mater.* **2016**, *28*, 6591−6604.
(26) Gao, B.; Liu, L.; Liu, J.; Yang, F. Photocatalytic degradation of 2, 4, 6-tribromophenol on Fe_2O_3 or FeOOH doped $ZnIn_2S_4$ heterostructure: Insight into degradation mechanism. *Appl. Catal., B* **2014**, *147*, 929−939.
(27) Sun, S.; Li, H.; Xu, Z. J. Impact of surface area in evaluation of catalyst activity. *Joule* **2018**, *2*, 1024−1027.
(28) Luna, A. J.; Nascimento, C.A.O.; Chiavone-Filho, O. Photodecomposition of hydrogen peroxide in highly saline aqueous medium. *Braz. J. Chem. Eng.* **2006**, *23*, 341−349.
(29) Solís-López, M.; Durán-Moreno, A.; Rigas, F.; Morales, A. A.; Navarrete, M.; Ramírez-Zamora, R. M. Assessment of copper slag as a sustainable Fenton-type Photocatalyst for water disinfection. *Water Reclam. Sustainability* **2014**, 199−227.
(30) Hong, J.; Suzuki, N.; Nakata, K.; Terashima, C.; Kim, K.; Fujishima, A.; Katsumata, K. I. Hydrogen production using iron oxyhydroxide with light irradiation. *Renewable Energy* **2021**, *164*, 1284−1289.
(31) Yamada, T.; Suzuki, N.; Nakata, K.; Terashima, C.; Matsushita, N.; Okada, K.; Katsumata, K. I.; et al. Hydrogen production system by light-induced α-FeOOH coupled with photoreduction. *Chem. − Eur. J.* **2020**, *26*, 2297.
(32) Bauer, R.; Waldner, G.; Fallmann, H.; Hager, S.; Klare, M.; Krutzler, T.; Malato, S.; Maletzky, P. The photo-fenton reaction and the TiO2/UV process for waste water treatment− novel developments. *Catal. Today* **1999**, *53*, 131−144.
(33) Chen, Y. C.; Lin, Y. G.; Hsu, Y. K.; Yen, S. C.; Chen, K. H.; Chen, L. C. Novel iron oxyhydroxide lepidocrocite nanosheet as ultrahigh power density anode material for asymmetric supercapacitors. *Small* **2014**, *10*, 3803−3810.
(34) Zhao, Y.; Jiangyong, H.; Chen, H. Elimination of estrogen and its estrogenicity by heterogeneous photo-Fenton catalyst β-FeOOH/resin. *J. Photochem. Photobiol., A* **2010**, *212*, 94−100.
(35) Machulek, A., Jr.; Frank, H.; Fabio, G.; Silva, V. O.; Friedrich, L. C.; Moraes, J.E.F. Fundamental Mechanistic Studies of the Photo-Fenton Reaction for the Degradation of Organic Pollutants. In *Organic Pollutants Ten Years after the Stockholm Convention-Environmental and Analytical Update*; InTech, 2012.

https://doi.org/10.1021/acsomega.1c04251
ACS Omega 2021, 6, 30562−30568